AIAA JOURNAL
Vol. 33, No. 1, January 1995

Asymptotic Velocity Defect Profile in an Incipient-Separating Axisymmetric Flow

Rakesh K. Singh* and Ram S. Azad†
University of Manitoba, Winnipeg, Manitoba R3T 2N2, Canada

Presence of a new asymptotic mean velocity profile (velocity defect law) was found concomitant with appreciable incipient separation (instantaneous detachment $\geq 20\%$ of the time) and extremely high-turbulence intensities in the final stages of an 8-deg total divergence angle conical diffuser fed with a fully developed turbulent pipe flow. Pulsed-wire anemometry was used for the measurement of incipient flow separation, mean velocities and skin-friction distributions. The conical diffuser flow shows some attributes of quasiequilibrium in the final one-third length. In the second-half of the diffuser the mean velocity profiles indicate a distinct point of inflection, the wall regions have less sensitivity to the initial conditions, and the flow exhibits some insensitivity toward the local boundary conditions. A comparison with the other asymptotic velocity defect profiles in Perry-Schofield coordinates revealed the distinctly different shape of the present asymptotic profile found in the conical diffuser. The validity of this asymptotic mean velocity profile was confirmed at two Reynolds numbers. Application of rapid distortion theory indicated coexistence of the regions of slowly and rapidly changing turbulence in the conical diffuser. Results of the present study also support the theory that turbulence is not universal and depends on the initial and boundary conditions.

I. Introduction

AXISYMMETRIC turbulent flow separation in a conical diffuser is an important problem in many practical flows. To tackle the extremely challenging problem of turbulent separation one must understand how a severe adverse pressure gradient (APG) distorts the development of the boundary layer. It is also important to know flow insensitivity toward the initial and local boundary conditions. In a conical diffuser, the flow is subjected to sudden perturbations of severe APG, extra strain rates, and streamline curvature. Hence, a conical diffuser flow is suitable for investigating the wall layer growth and separation in axisymmetric flows. To develop and validate closure models for conical diffuser flows it is necessary to have high-quality empirical data obtained using the appropriate new techniques such as pulsed-wire anemometry,[1,2] laser-Doppler methods,[3,4] or flying hot-wire anemometry. Because of optical limitations, such as the refractive effects of the containment wall, it is difficult to use laser-Doppler anemometry in a conical diffuser flow. Further, the geometry of the flow restricts the application of flying hot-wire in a conical diffuser. In the present study, pulsed-wire anemometry has been used to obtain some new information about the mean flowfield and incipient flow separation. Some preliminary results of the present investigation have already been presented by Singh and Azad.[5,6] Here, we summarize these and present a subset of extensive mean-flow data to study the characteristics of an asymptotic mean velocity defect profile found in the final stages of a conical diffuser flow.

According to Sovran and Klomp,[7] an 8-deg conical diffuser with an area ratio 4:1 has optimum pressure recovery and highest effectiveness. This optimum-performance geometry was selected for the present investigation. The results are presented for two Reynolds numbers, 6.9×10^4 (case I) and 1.2×10^5 (case II), based on the mean bulk velocity U_{bi} and the inside diameter D_i of the pipe. Although this is not a wide range we do believe that the present asymptotic mean velocity profile will exist even at high Reynolds numbers as the characteristics of conical diffuser flow do not change significantly with Reynolds number.[8,9]

Several researchers[4,10,11] have postulated that APG turbulent boundary-layer flows have an asymptotic nature of velocity profiles near separation. The present investigation revealed the existence of a new asymptotic velocity defect law in the final stages of an incipient-separating conical diffuser flow. This asymptotic velocity defect law was detected by plotting the mean velocity profiles obtained at various stations in the diffuser on Perry-Schofield[12] coordinates. The main objective of the present investigation is to critically examine the development of this asymptotic velocity profile found in the conical diffuser, to increase the understanding of highly turbulent incipient-separating axisymmetric flows. Comparisons with the other nearly separating flows, developing under different pressure gradients and flow configurations are also presented. Accurate prediction of the asymptotic velocity defect law will be a good test for evaluating the performance of models for the conical diffuser flows.

II. Experimental Apparatus and Method

The wind-tunnel facility used for the present study has been described previously.[5,8,9] Briefly, the wind is blown through the settling chamber and a circular contraction cone of nominal area ratio 87:1 and a 74-diam-long smooth steel pipe of inside diameter $D_i = 0.1016$ m. To achieve a fully developed turbulent pipe flow at the exit of the pipe, the first 1 diameter length of pipe from its inlet end was pasted with no. 16 floor-sanding paper. The resulting pipe flow was fed to an 8-deg nominal total angle conical diffuser which discharges free to the atmosphere. The plexiglas conical diffuser has inlet and outlet diameters of 0.1016 and 0.202 m, respectively, thus having a nominal area ratio of 4:1 over its length of 0.745 m. Figure 1 presents the geometry of the conical diffuser and the positions of the available stations for measurements. Each of the nine stations has eight equally spaced drilled holes on the periphery of the diffuser wall and two plugs for each hole. The plugs have central holes suitable for positioning wall static pressure tap tubing and a pulsed-wire wall shear stress probe. The inside surface of the plugs were aligned and curved flush with the inner surface of the diffuser wall.

Based on the level of measured instantaneous flow reversals at 0.05 mm above the wall, the conical diffuser flow has been divided into three stages or regions, namely, the initial stage, $x \approx 0.0$–0.15 m (instantaneous backflow up to 1% of the time), where x is the axial distance from the entrance of the conical diffuser measured in the downstream direction; the intermediate stage, $x \approx 0.15$–0.40 m (instantaneous backflow 1–20% of the time); and the final stage, $x \approx 0.40$–0.745 m (instantaneous backflow 20–30% of the time).

Received Nov. 24, 1993; revision received Aug. 22, 1994; accepted for publication Aug. 24, 1994.

*Graduate Research Assistant, Department of Mechanical and Industrial Engineering. Student Member AIAA.

†Professor of Fluid Mechanics, Department of Mechanical and Industrial Engineering. Member AIAA.

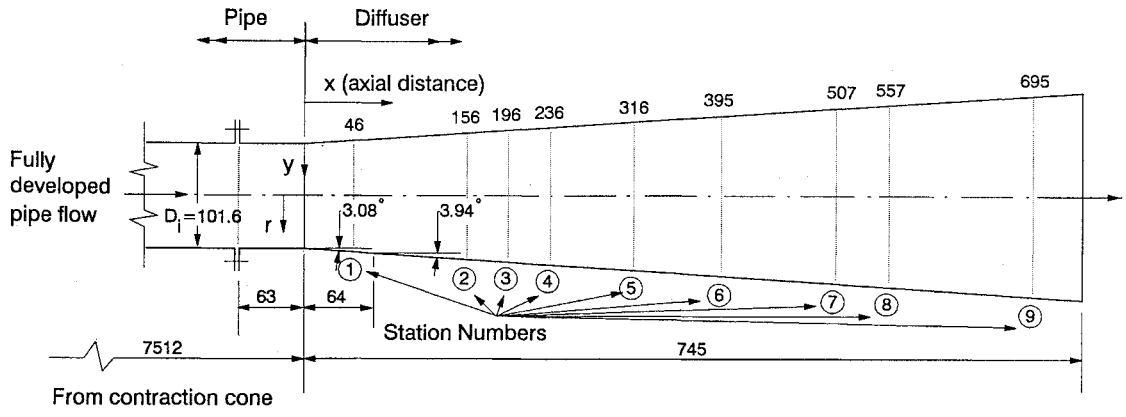

Fig. 1 Geometry of the conical diffuser and positions of measuring stations, dimensions in millimeters.

The axisymmetry and fully developed flow condition in the pipe was checked by Okwuobi and Azad.[8] The axisymmetry of the diffuser flow was checked by comparing long time mean values of turbulence quantities up to fourth moments as well as mean velocity at equal distances from the diffuser axis.

The traversing mechanism and the boundary-layer facility used for calibration of the pulsed-wire probes were described by Azad and Burhanuddin.[13] The usual Pitot and static pressure tubes were used with manometers for pressure measurements.[5] The hot-wire measurements were obtained using DANTEC equipment.[5] The hot-wire probes were operated at an overheat ratio of 0.8 with a measurement integration time of 60–120 s. The hot-wire data were corrected for yaw and high intensity of turbulence according to Champagne and Sleicher[14] and Vagt.[15] The x-wire Reynolds shear stress ($\overline{uv}$) data were also corrected for high intensity of turbulence according to Tutu and Chevray.[16] The experimental uncertainty in $\overline{uv}$ data is estimated to be ±15%.

Pulsed-wire data was used for the locations where incipient reversals occurred, or where the local turbulence intensity was high. Pulsed-wire measurements were obtained using PELA Flow Instruments pulsed-wire probes, and a PELA Flow Instruments anemometer interfaced to a microcomputer so that on-line calibrations and measurements could be made using a modified software. The standard pulsed-wire probes had platinum plated tungsten pulsed and sensor wires each of 5-μm nominal diameter and 10 mm length. The distance between the pulsed wire and sensor wires was approximately 1.2 mm. Standard pulsed-wire probes were calibrated in a low-turbulence freestream using Pitot and static pressure tubes and an empirical calibration curve of the form $U = (A/T) + (B/T^3)$, where U is the mean velocity, A and B are constants of calibration, and T is the time of flight of the heat tracer. In turbulent flow, up to 10,000 samples of time of flight were recorded at each location of measurement, using a sampling rate of 50–100 Hz.

Ruderich and Fernholz,[17] Dengel et al.,[18] and Dengel and Fernholz[11] have discussed the suitability of the pulsed-wire skin-friction measurement technique in various highly turbulent separating flows. Singh and Azad[6] have shown the limitations of the conventional Preston tube in the present flow. Therefore, the pulsed-wire technique was used for obtaining the wall shear stress distribution in the present diffuser flow. The experimental uncertainty in the pulsed-wire mean wall shear data is estimated to be ±10%. The pulsed-wire skin-friction probe was calibrated in terms of surface kinematic shear stress (τ_w/ρ) against a Preston tube in a well-documented turbulent boundary layer flow.[13] The calibration of Patel[19] was used for the Preston tube data and a good calibration fit was obtained using the relation $(\tau_w/\rho) = (A/T) + (B/T^2) + (C/T^3)$, where τ_w is the mean wall shear stress; ρ is the density of the air; A, B, and C are calibration constants; and T is the time of flight of the heat tracer. For wall shear stress measurement at each station, 3000–5000 samples of time of flight were taken at a sampling rate of 10–50 Hz. The hot-wire and pulsed-wire calibrations were repeated before and after each profile measurement, and the data were rejected if the calibration changed by more than 1.5%. The accuracy of the mean velocity profiles was checked by applying integral constraint of continuity at x-stations in the diffuser and the mass flow rates at different stations varied within 3% as compared to the mass flow rate in the pipe at the diffuser inlet.

III. Experimental Results and Discussion

A. Integral Quantities

Figure 2 illustrates the development of the wall static pressure recovery coefficient C_p defined as $C_p \equiv \{P_{sw}(x) - P_{sw}(\text{pipe})\}/(0.5\rho U_{bi}^2)$, where $P_{sw}(x)$ is the wall static pressure at various x locations and $P_{sw}(\text{pipe})$ the wall static pressure in the pipe at $x = -0.025$ m. The distribution of C_p shows the usual trend expected in an APG flow. Figure 2 also shows the distribution of the nondimensional inner pressure gradient parameter $P^+ = (\nu/u_*^3)(1/\rho)(dP_{sw}/dx)$, where ν is the kinematic viscosity and u_* the friction velocity obtained using the pulsed-wire skin-friction probe. The rising trend and very high values of parameter P^+ show the increasing severity of the pressure gradient and its effect in the wall region as the flow moves downstream in the conical diffuser. The scatter in the values of the parameter P^+ in the latter stages may be due to very small values of friction velocities and appreciable errors associated with them. The distribution of the parameter P^+ in the conical diffuser in Fig. 2 may be considered the same for both cases I and II, within experimental uncertainties.

Distributions of the displacement thickness δ^*, momentum thickness θ, energy thickness δ^{**}, and the shape factors $H = \delta^*/\theta$ and $H' = \delta^{**}/\theta$ were obtained using appropriate axisymmetric definitions.[7] These parameters were found to have trends similar to those reported by other researchers in conical diffuser and boundary-layer flows.[6] Parameters H and δ^* consistently increase in the diffuser, whereas θ and δ^{**} increase in the initial region and remain nearly constant in the final stages. The shape parameter H' reduces in the initial stages and remains nearly constant in the intermediate and final stages. It was found that δ^* grows to over eight times its entry value in the diffuser, whereas θ increases to only about two and one-half times its initial value.[6] This resulted in an increase of shape parameter H to over three times its entry value in the conical diffuser. Present results corroborate the observations in APG boundary-layer flows that a rapid increase of δ^* is a characteristic of flows approaching separation. The momentum thickness Reynolds number $Re_\theta = U_{cL}\theta/\nu$, where U_{cL} is the local centerline velocity, increases in the initial stages and remains approximately constant in the latter-half of the present diffuser. Nearly asymptotic behavior of the parameters δ^{**}, H', and Re_θ in the final stages of the present conical diffuser shows a state of quasiequilibrium for the flow in this region and corroborates the development of an asymptotic velocity defect law in this part of the conical diffuser.

According to Schofield[20] APG equilibrium layers require a freestream velocity variation of the form $U_1 = A(x - x_0)^m$, $m < 0$, where exponent m is a measure of the severity of the pressure gradient applied to the flow, x_0 an effective origin, and A a constant. In a two-dimensional APG boundary-layer flow maintained just at the condition of mean-flow separation, Stratford[21] suggested $m = -0.25$, assuming a value of $H = 2.0$. The corresponding value for equilibrium laminar layers is $-m = 0.0904$ (Ref. 22). For a two-dimensional equilibrium turbulent boundary layer, Cutler and

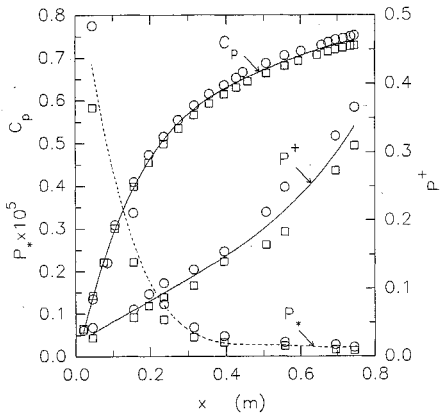

Fig. 2 Distribution of wall static pressure coefficient C_p and nondimensional pressure gradient parameters P^+ and P_* in conical diffuser. ○ $Re = 6.9 \times 10^4$ (case I) and □ $Re = 1.2 \times 10^5$ (case II), lines merely indicate the interpreted trend.

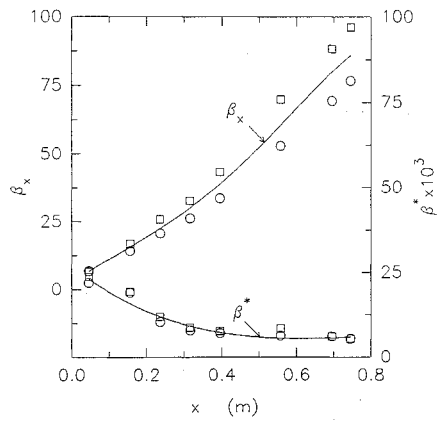

Fig. 3 Development of Clauser pressure gradient parameter β_x and Schofield nondimensional force ratio β^* in conical diffuser. Symbols as in Fig. 2; lines merely indicate the interpreted trend.

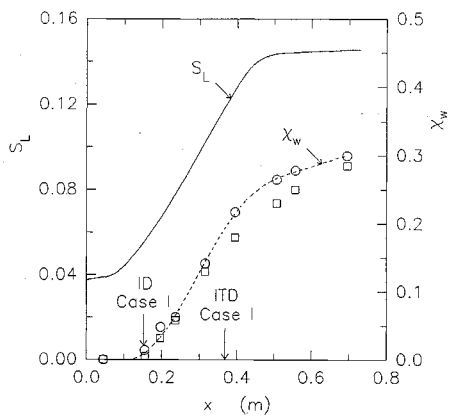

Fig. 4 Relative strength of large eddies S_L and reverse-flow parameter χ_w in conical diffuser. ID and ITD indicate the location of incipient detachment and intermittent transitory detachment, respectively; symbols as in Fig. 2; lines merely indicate the interpreted trend.

Johnston[23] have recently reported $m = -0.27$. Fitting a power law of the form $U_{cL} = A(x - x_0)^m$ to the centerline velocities in the present conical diffuser resulted in $m \approx -0.38$ and -0.43, for cases I and II, respectively. In the region of the asymptotic velocity defect profile, the measured axial pressure gradients dP_{sw}/dx were fitted with a power law of the form $dP_{sw}/dx = A(x - x_0)^m$ and resulted in $m \approx -0.45$ and -0.53, for cases I and II, respectively. The higher negative values of the exponent m in the present diffuser flow as compared to the two-dimensional APG flows[21,23] indicate that conical diffuser flows can withstand a considerably greater pressure gradient without mean-flow separation.

In a severe APG two-dimensional diffuser flow, Stratford[24] pointed out that the mean velocity profiles near the wall did not contain a logarithmic region but correlated instead with a half-power law (i.e., $U \propto y^{\frac{1}{2}}$). According to Schofield,[20] in moderate to strong APG flows where u_* is relatively small and of minor importance, the velocity scale of the logarithmic regions u_* should be replaced by U_s, the velocity scale of the half-power region. The velocity scale U_s of the half-power region is in fact a wall slip velocity,[10] and U_s can be found by extrapolating the half-power law to the wall in the plot of U/U_1 vs $(y/\delta^*)^{\frac{1}{2}}$. Trupp et al.[25] have shown the existence of half-power law regions and the absence of universal log-law regions for the mean velocity profiles at various axial stations in a similar geometry conical diffuser. The pulsed-wire data indicate very small values of u_* in the present conical diffuser. These results would suggest U_s to be the appropriate velocity scale in the present flow. For these reasons, the parameter P^+ seems inappropriate for the present flow as it is based on $1/(u_*)^3$. As pointed out by a referee, a new nondimensional pressure gradient parameter $P_*[= (\nu/\rho U_s^3)(dP_{sw}/dx)]$ was calculated based on the velocity scale U_s and its distribution for the present conical diffuser is shown in Fig. 2. This parameter seems appropriate for moderate to severe APG flows. The slowly changing behavior of P_* in the latter part of the diffuser indicates the quasiequilibrium nature of the flow.

Schofield[20] pointed out that Clauser's[26] original nondimensional force ratio or pressure gradient parameter, $\beta_x = (\delta^*/\tau_w)(dP_{sw}/dx)$, is inappropriate for the flows in moderate to strong APG with relatively small values of u_*; and the relevant pressure gradient parameter is β^*, defined as $\beta^* = (\delta^*/\rho U_s^2)(dP_{sw}/dx)$. The distribution of parameters β_x and β^* was calculated in the present diffuser for comparison purposes and results are presented in Fig. 3. It can be seen that the Clauser parameter β_x has a consistent rising trend in the diffuser for cases I and II, whereas the parameter β^* decreases in the initial stages and achieves nearly a constant value in the final stages. The distribution of parameter β^* supports the development of an asymptotic profile in the final stages of the present diffuser. These results of the pressure gradient parameters corroborate the usefulness of the velocity scale U_s in severe APG flows.

Azad and Kassab[27] have presented the distribution of the relative strength of large eddies S_L in a similar geometry conical diffuser in their Fig. 10b. The relative strength S_L is defined as $S_L \equiv (\overline{q^2 v}_{max} - \overline{q^2 v}_{min})/(\overline{q^2_{max}})^{\frac{3}{2}}$, where the resultant intensity $\overline{q^2} \equiv \overline{u^2} + \overline{v^2} + \overline{w^2}$ (2×, turbulent energy); $\overline{q^2 v} \equiv \overline{u^2 v} + \overline{v^3} + \overline{v w^2}$; u, v, and w are the components of the velocity fluctuations and max implies maximum with respect to y at x-station. The distribution of S_L is presented in Fig. 4, for comparison purposes. Based on the asymptotic nature of S_L in the final stages of the diffuser, in Ref. 27 it is concluded that an equilibrium large-scale structure exists in the final period of the diffuser flow. This behavior of S_L supports the development of an asymptotic mean velocity profile in the latter part of the conical diffuser.

The pulsed-wire technique can be used to quantitatively measure instantaneous flow reversals in terms of the reverse-flow parameter χ, defined as the fraction of time that the flow moves in an upstream direction, and measured as the ratio of the samples with a negative sign and the sum of all valid samples.[17] In the conical diffuser the wall value of the reverse-flow parameter χ_w was measured by the pulsed-wire wall probe at $y \approx 0.05$ mm above the wall, and its distribution is shown in Fig. 4. It can be seen that instantaneous reversals begin somewhere near $x = 0.14$ m at the wall and grow as the flow moves toward the diffuser exit. At station 2 for case I, $x = 0.156$ m and $\chi_w \approx 0.01$, which corresponds to the position of incipient detachment (ID), according to Simpson et al.[4] Similarly, $\chi_w \approx 0.20$, at $x = 0.38$ m near station 6, is the position of intermittent transitory detachment (ITD). Figure 4 shows the locations of ID and ITD for case I in the present diffuser. The asymptotic profile exists in the region downstream from the location of ITD.

It may be noted that Simpson et al.[4] have specified the near-wall value of the instantaneous reverse flow (i.e., reverse-flow parameter χ_w) at 1.02 mm above the wall surface, whereas in the present study it is obtained at 0.05 mm from the wall. Station 9, $x = 0.695$ m, in the present diffuser[5] and station $x = 129.4$ in. in Simpson et al.[4] have comparable near-wall distributions of instantaneous flow reversals. The results obtained at these two stations were examined

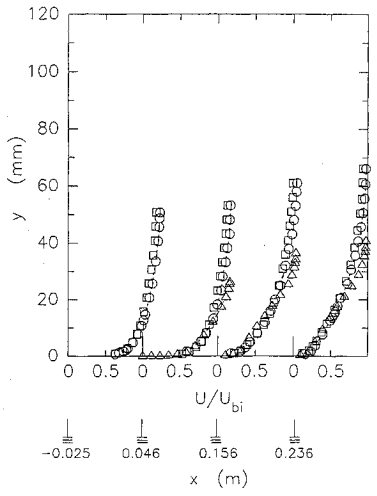

Fig. 5a Profiles of mean velocity from wall to centerline near pipe exit and at stations 1, 2, and 4 in conical diffuser. ○ present data, △ Thompson's[28] calculated profile (case I), and □ present data (case II).

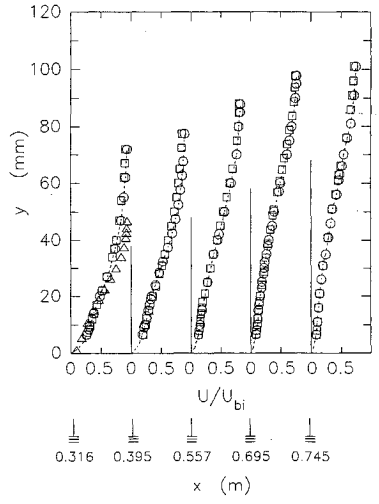

Fig. 5b Profiles of mean velocity from wall to centerline at stations 5, 6, 8, 9, and exit face in conical diffuser; symbols as in Fig. 5a.

to determine the extent of the discrepancies. At station 9, the 0.05-mm distance above the wall corresponds to $y^+ \approx 0.3$, $y/R_L \approx 0.0005$, where R_L is local radius, $y/\delta^* \approx 0.0013$, and $\chi = \chi_w(\approx 0.30)$; whereas the 1.02 mm distance above the wall results in $y^+ \approx 6.12$, $y/R_L \approx 0.0102$, $y/\delta^* \approx 0.0265$, and $\chi \approx 0.23$. In Simpson et al., at $x = 129.4$ in., the 1.02-mm distance above the wall corresponds to $y^+ \approx 12$, $y/\delta \approx 0.0082$, $y/\delta^* \approx 0.0194$, and $\chi \approx 0.19$. It may be noted that at this station the nearest location, $y \approx 0.26$ mm, from the wall at which instantaneous backflow was measured indicate $\chi \approx 0.31$ (see Fig. 5 of Simpson et al.[4]). These results show the rapidly changing nature of χ in the near-wall region.

The instantaneous backflow increases rapidly as the wall is approached in the conical diffuser.[5,6] For example, at station 9 for case I, $\chi \approx 0.09$ at about 6.5 mm from the wall, which increases to $\chi \approx 0.23$ near 1 mm above the wall, and to $\chi_w \approx 0.30$ at 0.05 mm above the wall. This shows the steepness of gradient $d\chi/dy$ in the near-wall region. Similar to Dengel and Fernholz,[11] at various stations of the present diffuser, the profiles of parameter χ obtained by traversing a pulsed-wire velocity probe were extrapolated to the respective wall value χ_w (Refs. 5 and 6). These profiles (not shown here for conciseness) indicated that the ITD location, which is near station 6, $x = 0.395$ m, when instantaneous flow reversals are detected at 0.05 mm above the wall, would be near station 8, $x = 0.557$ m, if χ_w were obtained at 1.02 mm above the wall (e.g., in Simpson et al.[4]). These results indicate that there may be appreciable differences in the locations of ID and ITD depending on the near-wall location of measurement.

In the present conical diffuser, the relative strength of large eddies S_L and parameter χ_w show a similar trend, illustrating their connected nature (see Fig. 4). The slowly changing characteristics of parameters S_L and χ_w in the final stages of the diffuser also corroborate the development of an asymptotic velocity defect profile in this region.

B. Mean Velocity Profiles

Figures 5a and 5b present the profiles of streamwise mean velocity obtained at various x stations in a nondimensional form. The first four profiles, shown in Fig. 5a, do not show any point of inflection; whereas, the profile obtained at station 5, $x = 0.316$ m, and the profiles at farther downstream stations, presented in Fig. 5b, show increasing evidence of inflection as the profile distances increase from the diffuser inlet. The plots of the mean velocity profiles in the near-wall coordinates indicated that the standard log-law is not applicable in this diffuser flow.

Thompson[28] reported a new family of mean velocity profiles for turbulent boundary-layer flows based on the combination of two universal functions representing the effects of the wall and of the intermittency in the outer region. None of the measured profiles in the diffuser show agreement with Thompson's calculated profiles (see Figs. 5a and 5b). This could be expected as these profiles were developed for moderate APG two-dimensional flows and Thompson himself indicated that the two-parameter family gives poor agreement with experimental data in the regions of severe APG and small surface shear, e.g., in the flow of Stratford,[24] where universal logarithmic law of the wall does not hold and parameter $P^+ > 0.01$. In the present diffuser, the parameter P^+ has very large values (≈ 0.03–0.36) and the universal log-law is not valid. In Fig. 5b, Thompson's profiles could not be obtained for the stations in the latter-half of the diffuser due to very high values of H (>3.0) in the present diffuser, for which Thompson's charts of y/θ contours for U/U_1 in the H vs $\log_{10} Re_\theta$ plots are not available.

Based on the findings of Schofield and Perry,[29] Perry and Schofield[12] reported that in two-dimensional APG flows, which satisfy the condition $(|\overline{uv}|_{\max}/u_*^2) \geq 1.5$, the mean velocity profiles collapsed onto a velocity defect law in $(U_1 - U)/U_s$ vs y/B coordinates, where U_s is a velocity scale characteristic of the outer flow, and B is a length scale. Okwuobi and Azad,[8] Azad and Hummel,[9] Azad and Kassab,[27] and Trupp et al.[25] have shown various similarities of the conical diffuser flow with other APG flows. As discussed earlier, the mean velocity profiles in the present diffuser show half-power regions and the velocity scale U_s seems the appropriate scale for this flow. These results would indicate the possibility of getting the asymptotic nature of the velocity defect profile for conical diffuser flows in Perry-Schofield coordinates which are based on the velocity scale U_s. The original relationships of the Perry-Schofiled similarity scales were used for the conical diffuser flow to follow the method of obtaining U_s outlined by Schofield and Perry.[29] This was also to facilitate the comparison of the mean velocity profiles of different flows, nondimensionalized in a similar manner and presented in a well-known coordinates system. Replacing the freestream velocity U_1 by centerline velocity U_{cL} the Perry-Schofield defect law for the mean velocity profile may given as

$$(U_{cL} - U)/U_s = 1 - 0.4(y/B)^{\frac{1}{2}} - 0.6\sin(\pi y/2B) \qquad (1)$$

where B is the integral layer thickness, defined as $B = 2.86\delta^* U_{cL}/U_s$, U_{cL} is the local centerline velocity, and U_s is a scaling velocity based on a half-power profile. In the wall region Eq. (1) may be presented in the half-power form as

$$U/U_{cL} = 0.47(U_s/U_{cL})^{\frac{3}{2}}(y/\delta^*)^{\frac{1}{2}} + 1 - (U_s/U_{cL}) \qquad (2)$$

The velocity ratio U_s/U_{cL} can be obtained from the measured mean velocity profiles by applying Clauser's[26] methodology to Eq. (2). The velocity scale U_s is related to the maximum shear stress velocity U_m using the relation

$$U_s/U_m = 8.0(B/L)^{\frac{1}{2}} \qquad (3)$$

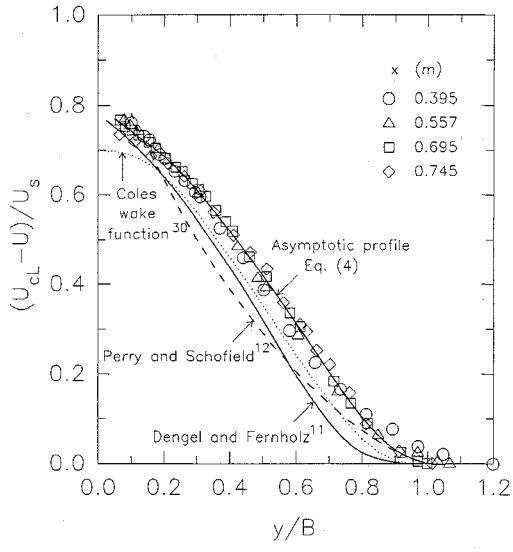

Fig. 6 Mean velocity profiles in Perry-Schofield coordinates, Re = 6.9×10^4 (case I).

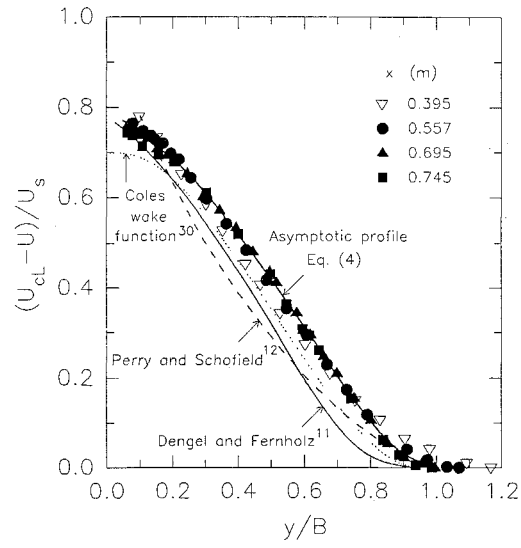

Fig. 7 Mean velocity profiles in Perry-Schofield coordinates, Re = 1.2×10^5 (case II).

where $U_m = (|\overline{uv}|_{max})^{\frac{1}{2}}$ and L is the distance from the wall to the position of U_m. Equation (3) is important as it relates the mean-flow parameters to the turbulent-flow parameters.

The mean velocity data obtained at various stations of the diffuser were plotted on Perry-Schofield[12] coordinates, and we found that none of the resulting profiles fit the Perry-Schofield velocity defect, Eq. (1). However, these coordinates were found useful as the velocity profiles for station 8, $x = 0.557$ m, station 9, $x = 0.695$ m, and the exit face $x = 0.745$ m collapse very well on a single asymptotic curve for both cases I and II, as shown in Figs. 6 and 7. Each of the other velocity profiles for the upstream stations 1–5 were distinctly different and could not be fitted with any common curve. Figures 6 and 7 show that the mean velocity data for station 6 $x = 0.395$ m results in a profile which is only slightly different from the given asymptotic profile for stations 8, 9, and the exit face, for both cases I and II. Hence, the asymptotic profile exists for the final one-third length of the present diffuser, in the flow regime downstream from station 6, where appreciable incipient reversals ($\chi_w \geq 0.2$) were detected in the wall region. This asymptotic outer-law mean velocity profile for the final stages of the conical diffuser can be fitted by a seventh-order polynomial

$$\frac{U_{cL} - U}{U_s} = \sum_{i=0}^{7} A_i (y/B)^i, \qquad 0.05 \leq y/B \leq 0.95 \qquad (4)$$

with the following values of the constants A_0 to A_7

$$A_0 = 0.811 \qquad A_1 = -1.012$$
$$A_2 = 5.639 \qquad A_3 = -29.747$$
$$A_4 = 72.407 \qquad A_5 = -95.044$$
$$A_6 = 64.157 \qquad A_7 = -17.208$$

Figures 6 and 7 show that this asymptotic profile for the conical diffuser flow is distinctly different as compared to the profile given by Perry and Schofield.[12] Figures 6 and 7 also include another asymptotic profile reported by Dengel and Fernholz[11] for an axisymmetric APG turbulent boundary-layer flow in the vicinity of separation. It can be seen that the asymptotic profile found in the final stages of the conical diffuser is distinctly different compared to the profile reported by Dengel and Fernholz.

According to Coles,[30] the development of a turbulent boundary layer can be interpreted in terms of an equivalent wake profile, and the flow at a point of separation is locally a pure wake flow. The law of the wake is characterized by the profile at a point of separation. This velocity-defect profile, known as Coles wake function, is also presented in Figs. 6 and 7 for comparison. According to Coles, at the condition of mean-flow separation $\delta^* = 0.5\delta$. Using the half-power

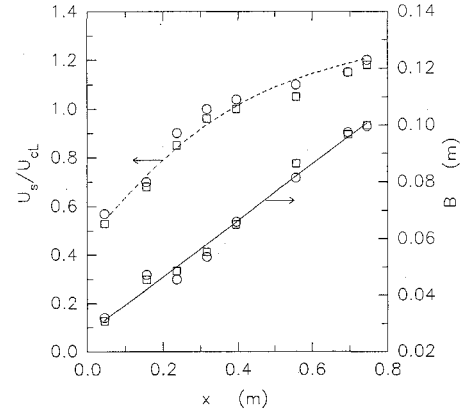

Fig. 8 Development of similarity velocity ratio and integral layer thickness. ○ Re = 6.9×10^4, □ Re = 1.2×10^5, $B = 2.86\delta^* U_{cL}/U_s$; lines merely indicate the interpreted trend.

law coordinates, the plot of Coles wake function resulted in $B \approx \delta$. It was found that the velocity profiles in the outer region of the diffuser flow do not have a universal wake function. Hence, the asymptotic velocity profile found in the conical diffuser is distinctly different as compared to the profiles according to Dengel-Fernholz,[11] Perry and Schofield,[12] and Coles[30] law of the wake. These results corroborate the observation of Schofield[10] that the degree of deviation from the standard Perry-Schofield correlation may probably be governed by the nature of the flow and the overall flow geometry.

It should be noted that the same asymptotic velocity profile fits for $Re = 6.9 \times 10^4$ (case I) and $Re = 1.2 \times 10^5$ (case II) in the final stages of the present conical diffuser (Figs. 6 and 7). It is believed that this asymptotic profile will be a valid representation of the mean velocity profiles in the final stages of conical diffuser flows with similar optimum geometries even at high Reynolds numbers, since the characteristics of diffuser flow do not show any remarkable Reynolds number dependence once the feed flow is fully developed and at sufficiently high Reynolds number.[8,9] The present study further illustrates the importance of Perry-Schofield coordinates for the mean velocity profiles. It seems that on these coordinates most of the severe APG flows may develop some asymptotic velocity defect law in the vicinity of separation.

Figure 8 presents the development of the similarity velocity ratio U_s/U_{cL} and Schofield-Perry integral layer thickness B in the conical diffuser. According to Schofield[20] for any equilibrium layer U_1/U_s is constant. Hence, a nearly asymptotic value of the ratio U_s/U_{cL} in the final stages of the diffuser shows a state of quasiequilibrium and corroborates the development of an asymptotic velocity defect profile. The distribution of the integral layer thickness B in the

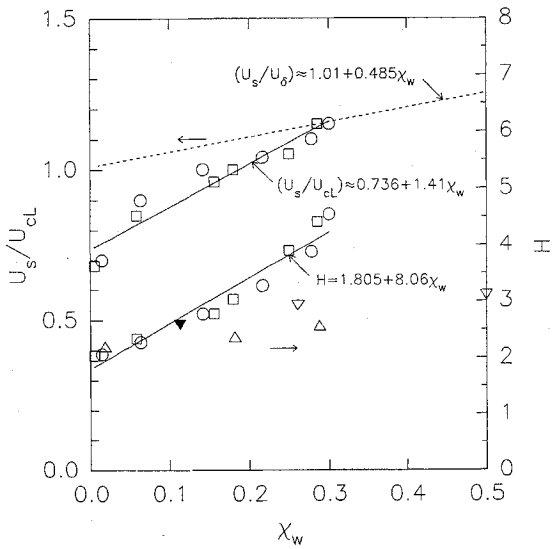

Fig. 9 Development of shape parameter H and velocity scale U_s/U_{cL} as a function of χ_w. ○ $Re = 6.9 \times 10^4$, □ $Re = 1.2 \times 10^5$, present data in diffuser; △ case 2, - - - - Dengel and Fernholz,[11] ▼ Simpson et al.,[3] ▽ Simpson et al.[4]

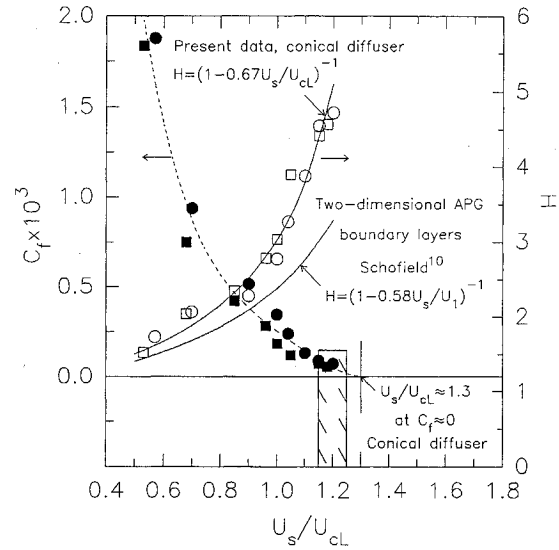

Fig. 10 Development of H and C_f as a function of velocity scale U_s/U_{cL} in conical diffuser, ● and ○ $Re = 6.9 \times 10^4$, ■ and □ $Re = 1.2 \times 10^5$, boxed hatched lines indicate the range of detachment condition for boundary layers according to Schofield,[10] - - - - interpreted trend of C_f vs U_s/U_{cL} in conical diffuser.

conical diffuser shows a linear growth similar to its characteristics found in other APG flows.[20]

Dengel and Fernholz[11] reported a linear relationship between the shape factor H and the reverse-flow parameter χ_w. The present results in a conical diffuser also give an approximately linear relationship between these two parameters as shown in Fig. 9. For both cases I and II, this relationship may be approximated as $H \approx 1.805 + 8.06\chi_w$ (in the range $0.01 < \chi_w < 0.30$). Figure 9 also includes H vs χ_w data of Simpson et al.[3,4] and Dengel and Fernholz,[11] for comparison purposes. It can be seen that in the initial stages of the diffuser, approximately up to $\chi_w \approx 0.12$, the data points of the diffuser flow are close to the data points of the other two flows.[3,4,11] In contrast, the values of the shape parameter H in the final stages of the conical diffuser are very high as compared to the other two flows,[3,4,11] due to axisymmetry, fully developed turbulent entry flow, and very high blockage in the present flow. It may be noted that the local blockage factor $B_L = 2\delta^*/R_L$ has very high values in the latter stages of the present diffuser.[6]

We also sought a linear relationship between the Schofield-Perry similarity velocity ratio U_s/U_{cL} and the reverse-flow parameter χ_w as reported by Dengel and Fernholz.[11] As expected, we did not get the same relationship as reported by those authors. However, we also found a linear relationship between these two parameters for the conical diffuser flow as shown in Fig. 9. The relationship reported by Dengel and Fernholz[11] is also included in Fig. 9 for comparison purposes. The relation between U_s/U_{cL} and the reverse-flow parameter χ_w for the conical diffuser flow may be given as $U_s/U_{cL} \approx 0.736 + 1.41\chi_w$ in the range $0.01 < \chi_w < 0.30$.

Schofield[10] reported wall shear stress distributions from two-dimensional boundary layers as a function of velocity ratio U_s/U_1. The detachment condition was given as $1.15 < U_s/U_1 < 1.25$ (see Fig. 10). Figure 10 shows a C_f vs U_s/U_{cL} plot for the present axisymmetric diffuser flow; where $C_f = \tau_w/(0.5\rho U_{cLi}^2)$ and U_{cLi} is the centerline velocity at the diffuser inlet. The approach of Schofield seems to be a correct one, since the velocity ratio U_s/U_{cL} in the conical diffuser results in a value of nearly 1.30 by extrapolation to $C_f = 0$, at the condition of mean-flow separation. Schofield also pointed out that the similarity velocity ratios have higher values, $1.2 < U_s/U_1 < 1.3$, for the reattaching layers after a separation bubble. In an axisymmetric flow, Dengel and Fernholz[11] reported $U_s/U_\delta \approx 1.25$, at the condition of mean separation $\chi_w \approx 0.5$; and $U_s/U_\delta \approx 1.35$ in the separated region with $\chi_w \approx 0.7$, where U_δ is the streamwise mean velocity at the edge of the boundary layer. These results show that the values of the similarity velocity ratio are slightly different depending on the flow configuration.

Schofield[10] indicated that there is a single H vs U_s/U_1 relation applicable to all attached and separated two-dimensional layers. It was suggested that the universal mean velocity profile at detachment has a similarity velocity ratio near 1.2, which results in $H = 3.3$. Schofield gave the following relationship for such flows, $H = (1 - 0.58U_s/U_1)^{-1}$. In the axisymmetric conical diffuser flow, we found a similar relationship with a different constant. This relationship may be expressed as $H = (1 - 0.67U_s/U_{cL})^{-1}$. Figure 10 shows plots of these two relationships applicable for two-dimensional boundary-layer flows and axisymmetric diffuser flows, respectively. In the present conical diffuser, the asymptotic velocity profile develops in the final stages, in the region where $U_s/U_{cL} > 1.0$ and the shape factor $H > 3.2$.

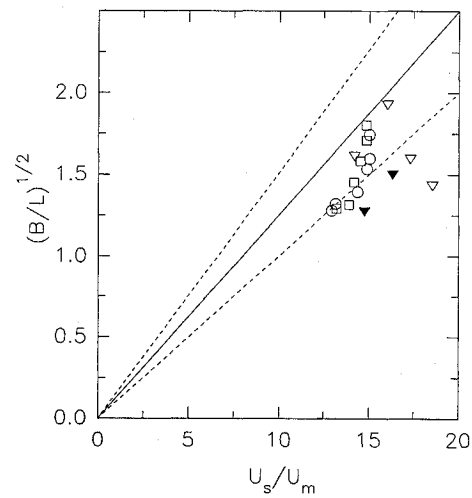

Fig. 11 Relation between mean-flow parameters and shear stress profile in conical diffuser. ○ $Re = 6.9 \times 10^4$, □ $Re = 1.2 \times 10^5$, dashed lines indicate the scatter limits for attached data according to Schofield,[10] ▼ Simpson et al.,[3] ▽ Simpson et al.[4]

Figure 11 presents the relation between the mean flow parameters (U_s and B) and the shear stress profile (U_m and L) in the present diffuser. The relation between the velocity scale U_s and the maximum shear stress velocity U_m and the scatter limits for the attached data according to Schofield[10] are also shown. The data of Simpson et al.[3,4] are included for comparison purposes. It can be seen that the relationship of the mean-flow parameters with the turbulent-flow parameters in the conical diffuser has a nature similar to that in APG boundary layers.

C. Integral Length Scales

To describe the structure of a turbulent flowfield it is essential to know the length scale of turbulence. The Eulerian longitudinal integral length scale L_f is considered to represent the streamwise

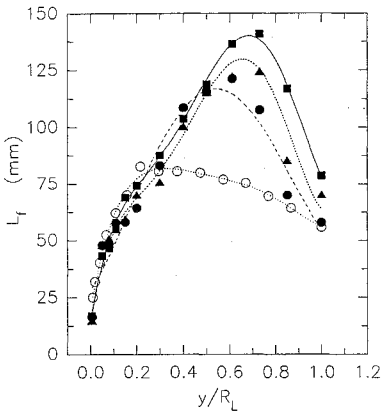

Fig. 12 Distribution of streamwise integral length scale L_f in pipe and conical diffuser. $Re = 1.2 \times 10^5$ (case II), ○ pipe, • station 6, ▲ station 8, ■ station 9; lines merely indicate the interpreted trend.

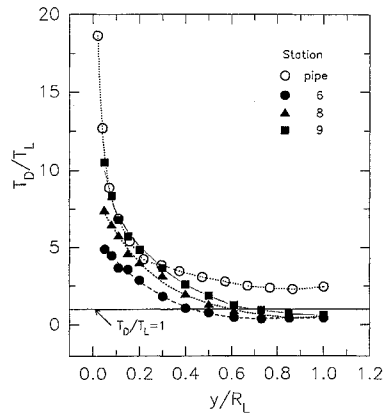

Fig. 13 Distribution of the ratio of travel time T_D to integral time scale T_L at pipe exit and in conical diffuser. $Re = 1.2 \times 10^5$ (case II); dashed lines for visual aid only.

scale of the energy containing eddies. The distribution of L_f was obtained in the pipe and at the three selected stations in the conical diffuser from the one-dimensional energy spectrum $E_1(k_1)$, using the relation $L_f = \lim_{(k_1 \to 0)} \pi E_1(k_1)/(2u^2)$, where k_1 is the wavenumber. The profiles of L_f in the pipe, and at stations 6, 8, and 9 in the diffuser, are presented in Fig. 12. The uncertainty of each data point is estimated as being in the order of ±8%. These profiles were calculated from the hot-wire spectra data reported by Azad and Kassab[31] for a similar geometry conical diffuser. It can be seen that the large eddies in the diffuser flow are continuously elongated in the direction of the flow in the initial stages, whereas the increase in length scales slows down in the final stages. The increase in the length scale L_f with the flow moving in the downstream direction indicates a growth of the turbulence structure.

According to rapid distortion theory (RDT), turbulent flows can be classified into rapidly changing and slowly changing in terms of their initial and boundary conditions.[32] If the travel time T_D (equal to the ratio of the distance along the streamline of the mean flow through the turbulent flow domain L_D to the local mean velocity U) of a fluid element within the turbulent flow domain is much greater than the memory time T_L (equal to the ratio of integral length scale L_f to the local rms velocity of the turbulence u'), it might be expected that the turbulence would become approximately independent of the initial condition. The ratio T_D/T_L can be used to divide the turbulent flows into the flows with rapidly changing turbulence (RCT) when $T_D/T_L \ll 1$ and slowly changing turbulence (SCT) when $T_D/T_L \geq 1$.

Figure 13 presents the distribution of the ratio T_D/T_L for three selected stations 6, 8, and 9 for case II, considering the pipe exit face as the reference condition. It can be seen that the value of the ratio $T_D/T_L < 1$ in the core region, indicating that the turbulence in the core region at these three stations of the conical diffuser will be sensitive to the initial conditions. Therefore, the core region in the final stages of the present diffuser can be classified as a region of RCT. In the wall regions at stations 6, 8, and 9 the ratios T_D/T_L are appreciably larger than unity, indicating that the wall regions at these stations would become partially independent or less sensitive to the initial conditions and can be classified as the regions of SCT.

These results corroborate the findings of Hunt and Carruthers[32] that in most turbulent flows the ratio $T_D/T_L \leq 1$ in the interior of the flow and $T_D/T_L \geq 1$ near the wall. The slowly changing nature of the wall layer in the final stages of a conical diffuser is also supported by other measurements such as slower increase in the level of instantaneous flow reversals, movement of peak production away from the wall, and nearly asymptotic behavior of various flow parameters such as β_* and P_* in the latter part of the diffuser. A fully developed turbulent flow in a pipe far from the entry should be independent of the incoming turbulence.[32] Figure 13 shows the distribution of T_D/T_L at the pipe exit, calculated taking the pipe entry face as the reference location. As expected, in the central and wall region of the pipe flow the values of T_D/T_L are appreciably larger than unity, indicating a fully developed turbulent flow condition in the pipe at the diffuser inlet.

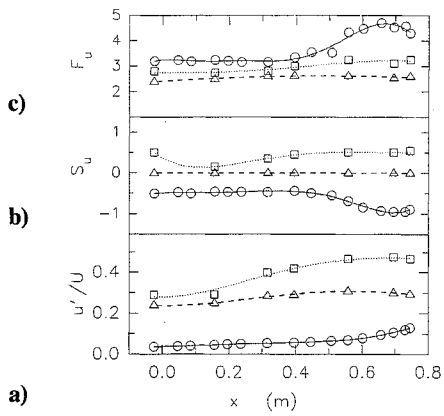

Fig. 14 Development of relative intensity u'/U, skewness factor S_u, and flatness factor F_u along conical diffuser. $Re = 6.9 \times 10^4$, ○ centerline, $\triangle\, y = y_{|\overline{uv}|\,\max}$, $\square\, y = (y_{|\overline{uv}|\,\max})/2$; lines for visual aid only.

Another criteria for a turbulent flow to be unaffected by the presence of the boundary is the ratio L_g/n, where L_g is the radial or vertical integral length scale and n the distance of the eddy from the boundary. The value of the ratio L_g/n determines whether or not the boundary affects the eddies. If $L_g/n \gg 1$, the turbulence is affected by the boundary conditions at a distance n. In the present diffuser flow at station 6 $x = 0.395$ m, according to the results of Azad and Hummel[9] for a similar geometry diffuser, the approximate range for the value of L_g is 8–14 mm, and the value of the local radius n is 80 mm. This results in values of L_g/n between 0.175 and 0.1, indicating that the turbulent flow will show some insensitivity toward the presence of the boundary at station 6 and farther downstream, as the value of n further increases at the downstream stations in the conical diffuser. These results support the development of the asymptotic mean velocity profile in the final one-third of the conical diffuser flow.

The development of the relative intensity of streamwise fluctuating velocity u'/U, where u' is the rms value of the fluctuating streamwise velocity; u; S_u, the skewness factors of u and F_u; the flatness factor of u, along the conical diffuser centerline, at $y = y_{|\overline{uv}|\,\max}$, and at $y = (y_{|\overline{uv}|\,\max})/2$ are presented in Figs. 14a, 14b, and 14c, respectively. The development of these quantities in the final stages of the diffuser flow also supports the classification of the core region as RCT and wall region as SCT. Figure 14a shows that in the final stages of the diffuser, downstream from station 6 $x = 0.395$ m the intensity u'/U in the core region increases almost two-fold; whereas the increase in u'/U in the wall region along the other two selected loci at $y = y_{|\overline{uv}|\,\max}$ and $y = (y_{|\overline{uv}|\,\max})/2$ is appreciably lower. Figure 14b illustrates that the S_u is essentially zero along

$y = y_{|\overline{uv}|\max}$, and it increases only slightly along $y = (y_{|\overline{uv}|\max})/2$. Similarly, in the final stages of the conical diffuser the profiles of F_u along the two selected loci in the wall region do not show remarkable variations, whereas the centerline values of S_u and F_u change dramatically especially in the final one-third of the conical diffuser (Figs. 14b and 14c). This behavior of u'/U, S_u, and F_u illustrates the conical diffuser core to be a region of RCT.

IV. Conclusions

1) Existence of a new asymptotic mean velocity defect profile has been found in Perry-Schofield coordinates in the final one-third length of the conical diffuser. This asymptotic profile exists in the downstream region from the location of intermittent transitory detachment (ITD).

2) The mean velocity profiles obtained in the second-half of the conical diffuser indicate a distinct point of inflection, illustrating the changing characteristics of the mean flow in the intermediate and final stages of the conical diffuser.

3) Application of some basic diagnostic aspects of the rapid distortion theory (RDT) revealed coexistence of the regions of rapidly changing turbulence (RCT) and slowly changing turbulence (SCT) at various stations of the conical diffuser. The central core region of the diffuser illustrates characteristics of RCT, whereas the wall regions were found to have attributes of SCT. The wall regions of the final stages in the diffuser indicate less sensitivity to the initial conditions. The diffuser flow also shows some insensitivity toward the local boundary conditions in the final stages.

4) The present study corroborates the relevance of Schofield pressure gradient parameter β^* and scaling velocity U_s for severe adverse pressure gradient incipient-separating flows with relatively small friction velocities. A new nondimensional pressure gradient parameter $P_* [= (\nu/\rho U_s^3)(\mathrm{d}P_{sw}/\mathrm{d}x)]$ is suggested for moderate to severe adverse pressure gradient flows. It was found appropriate to characterize the present conical diffuser flow using this parameter.

5) The relationship between the mean flow parameters (U_s and B) and Reynolds shear stress profile (U_m and L) in the conical diffuser was found to have similarity with the separating boundary-layer flow of Simpson et al.[3,4] Whereas the relationships between the shape parameter H and Perry-Schofield velocity scale U_s/U_{cL}, H and reverse-flow parameter χ_w, and χ_w and U_s/U_{cL} in the conical diffuser flow show different characteristics as compared to two-dimensional boundary-layer flows subjected to adverse pressure gradient.

6) A new relationship was found between Perry-Schofield velocity scale U_s/U_{cL} and the shape factor H for the axisymmetric flow in a conical diffuser. The parameters χ_w and H show a linear relationship. The parameters χ_w and U_s/U_{cL} also have a linear relationship in the conical diffuser. These relationships were found valid for both cases I and II.

Acknowledgments

The financial support of the Natural Sciences and Engineering Research Council of Canada is gratefully acknowledged. The authors express thanks to reviewers for valuable suggestionsand to S. W. Greenwood for thoroughly going through the original manuscript.

References

[1]Bradbury, L. J. S., and Castro, I. P., "A Pulsed-Wire Technique for Velocity Measurements in Highly Turbulent Flows," *Journal of Fluid Mechanics*, Vol. 49, Pt. 4, Oct. 1971, pp. 657–691.

[2]Castro, I. P., "Pulsed Wire Anemometry," *Experimental Thermal and Fluid Science*, Vol. 5, No. 6, 1992, pp. 770–780.

[3]Simpson, R. L., Strickland, J. H., and Barr, P. W., "Features of a Separating Turbulent Boundary Layer in the Vicinity of Separation," *Journal of Fluid Mechanics*, Vol. 79, Pt. 3, 1977, pp. 553–594.

[4]Simpson, R. L., Chew, Y.-T., and Shivaprasad, B. G., "The Structure of a Separating Turbulent Boundary Layer. Part 1: Mean Flow and Reynolds Stresses," *Journal of Fluid Mechanics*, Vol. 113, Dec. 1981, pp. 23–51.

[5]Singh, R. K., and Azad, R. S., "Measurement of Mean Velocity in a Complex Turbulent Flow," *Proceedings of the International Conference on Near-Wall Turbulent Flows*, edited by R. M. C. So, C. G. Speziale, and B. E. Launder, Elsevier, New York, 1993, pp. 629–638.

[6]Singh, R. K., and Azad, R. S., "Effects of Incipient Separation on the Mean and Turbulent Fluctuating Velocities in a Conical Diffuser Flow," *Proceedings of the Third World Conference on Experimental Heat Transfer, Fluid Mechanics and Thermodynamics*, edited by M. D. Kelleher, R. K. Shah, K. R. Sreenivasan, and Y. Joshi, Elsevier, New York, 1993, pp. 977–984.

[7]Sovran, G., and Klomp, E. D., "Experimentally Determined Optimum Geometries for Rectilinear Diffusers with Rectangular, Conical or Annular Cross-Section," *Fluid Mechanics of Internal Flows*, edited by G. Sovran, Elsevier, New York, 1967, pp. 270–319.

[8]Okwuobi, P. A. C., and Azad, R. S., "Turbulence in a Conical Diffuser with Fully Developed Flow at Entry," *Journal of Fluid Mechanics*, Vol. 57, Pt. 3, Feb. 1973, pp. 603–622.

[9]Azad, R. S., and Hummel, R. H., "Similarities of Turbulence Structure in a Conical Diffuser with Other Wall-Bounded Flows," *AIAA Journal*, Vol. 17, No. 8, 1979, pp. 884–891.

[10]Schofield, W. H., "Two-Dimensional Separating Turbulent Boundary Layers," *AIAA Journal*, Vol. 24, No. 10, 1986, pp. 1611–1620.

[11]Dengel, P., and Fernholz, H. H.,"An Experimental Investigation of an Incompressible Turbulent Boundary Layer in the Vicinity of Separation," *Journal of Fluid Mechanics*, Vol. 212, March 1990, pp. 615–636.

[12]Perry, A. E., and Schofield, W. H., "Mean Velocity and Shear Stress Distributions in Turbulent Boundary Layers," *Physics of Fluids*, Vol. 16, No. 12, 1973, pp. 2068–2074.

[13]Azad, R. S., and Burhanuddin, S., "Measurement of Some Features of Turbulence in Wall-Proximity," *Experiments in Fluid*, Vol. 1, 1983, pp. 149–160.

[14]Champagne, F. H., and Sleicher, C. A., "Turbulence Measurements with Inclined Hot- Wires, Part 2. Hot-Wire Response Equations," *Journal of Fluid Mechanics*, Vol. 28, Pt. 1, 1967, pp. 177–182.

[15]Vagt, J. -D., "Hot-Wire Probes in Low Speed Flow," *Progress in Aerospace Science*, Vol. 18, Pergamon, 1979, pp. 271–323.

[16]Tutu, N. K., and Chevray, R., "Cross-Wire Anemometry in High Intensity Turbulence," *Journal of Fluid Mechanics*, Vol. 71, Pt. 4, 1975, pp. 785–800.

[17]Ruderich, R., and Fernholz, H. H., "An Experimental Investigation of a Turbulent Shear Flow with Separation, Reverse Flow, and Reattachment," *Journal of Fluid Mechanics*, Vol. 163, Feb. 1986, pp. 283–322.

[18]Dengel, P., Fernholz, H. H., and Hess, M., "Skin-Friction Measurements in Two- and Three-Dimensional Highly Turbulent Flows with Separation," *Advances in Turbulence 1*, edited by G. Comte-Bellot and J. Mathieu, Springer, Berlin, 1987, pp. 470–479.

[19]Patel, V. C., "Calibration of the Preston Tube and Limitations on its Use in Pressure Gradients," *Journal of Fluid Mechanics*, Vol. 23, Pt. 1, Sept. 1965, pp. 185–208.

[20]Schofield, W. H., "Equilibrium Boundary Layers in Moderate to Strong Adverse Pressure Gradients," *Journal of Fluid Mechanics*, Vol. 113, Dec. 1981, pp. 91–122.

[21]Stratford, B. S., "The Prediction of Separation of the Turbulent Boundary Layer," *Journal of Fluid Mechanics*, Vol. 5, Pt. 1, Jan. 1959, pp. 1–16.

[22]Rotta, J., "Turbulent Boundary Layers in Incompressible Flow," *Progress in Aeronautical Sciences*, Vol. 2, edited by A. Ferri, D. Küchemann and L. H. G. Sterne, Pergamon, New York, 1962, pp. 1–219.

[23]Cutler, A. D., and Johnston, J. P., "The Relaxation of a Turbulent Boundary Layer in an Adverse Pressure Gradient," *Journal of Fluid Mechanics*, Vol. 200, March 1989, pp. 367–387.

[24]Stratford, B. S., "An Experimental Flow with Zero Skin Friction Throughout its Region of Pressure Rise," *Journal of Fluid Mechanics*, Vol. 5, Pt. 1, Jan. 1959, pp. 17–35.

[25]Trupp, A. C., Azad, R. S., and Kassab, S. Z., "Near-Wall Velocity Distributions within a Straight Conical Diffuser," *Experiments in Fluids*, Vol. 4, 1986, pp. 319–331.

[26]Clauser, F. H., "Turbulent Boundary Layers in Adverse Pressure Gradients," *Journal of the Aeronautical Sciences*, Vol. 21, Feb. 1954, pp. 91–108.

[27]Azad, R. S., and Kassab, S. Z., "Turbulent Flow in a Conical Diffuser: Overview and Implications," *Physics of Fluids A*, Vol. 1, No. 3, 1989, pp. 564–573.

[28]Thompson, B. G. J., "A New Two-Parameter Family of Mean Velocity Profiles for Incompressible Turbulent Boundary Layers on Smooth Walls," Aeronautical Research Council, Reports and Memoranda 3463, April 1965.

[29]Schofield, W. H., and Perry, A. E., "TheTurbulent Boundary Layer as a Wall Confined Wake," Aeronautical Research Labs, Australian Dept. of Defence, Mechanical Engineering Rept. 134, Feb. 1972.

[30]Coles, D.,"The Law of the Wake in the Turbulent Boundary Layer," *Journal of Fluid Mechanics*, Vol. 1, Pt. 2, July 1956, pp. 191–226.

[31]Azad, R. S., and Kassab, S. Z., "Spectral Data in Axisymmetric Wall-Bounded Shear Flow," Dept. of Mechanical Engineering, Rept. METR-4, Univ. of Manitoba, Winnipeg, Manitoba, Canada, 1985.

[32]Hunt, J. C. R., and Carruthers, D. J., "Rapid Distortion Theory and the 'Problems' of Turbulence," *Journal of Fluid Mechanics*, Vol. 212, March 1990, pp. 497–532.